An Electrical Infrastructure Management Model for Long-Term Maintenance and Hazard Mitigation

NATHANIEL M. LEVINE, KRISTEN HOLLINGSWORTH, YINGJIE WU, MORGAN GRIFFITH and BRIAN MCDONALD

ABSTRACT

Electrical lines are critical infrastructure components. Line failures can cause catastrophic wildfires resulting in immeasurable damage to life and property. This paper discusses the implementation of an electrical infrastructure management model that tracks component degradation over time and incorporates inspection and monitoring data to update the model; the model then identifies components with the highest risk of failure to direct maintenance operations and estimate long-term line performance. The capacity of the structures is represented through fragility curves based on first-principles modeling and industry standards. Threat models, such as metal corrosion and wood decay, estimate how the fragility curve will evolve with time, based on environmental data and the age of the structure. Data-driven approaches are used to incorporate field data and historical performance into the model. Bayesian updating is used to adjust the fragility curves based on historical wind and outage data. Similarly, observed deterioration from field condition inspections are applied to further modify the model. Using a site-specific hazard model, an annualized probability of failure is estimated for each structure on an electrical line. First, an overview of the framework is provided, with a specific focus on wind hazards. To illustrate the application of the model and illustrate the challenges encountered in implementation, an example case study is discussed, exploring how the predicted probabilities of failure can be impacted by the choice of wind hazard model. This choice can result in geographic bias towards both under- and over-predicting probability of failure, and therefore can result in misdirection of maintenance resources. Future planned improvements are discussed.

Nathaniel M. Levine, Senior Engineer, Email: nlevine@exponent.com. Buildings and Structures Practice, Exponent, Menlo Park, CA, USA.
Kristen Hollingsworth, Associate, Exponent, Menlo Park, CA, USA.
Yingjie Wu, Senior Engineer, Exponent, Menlo Park, CA, USA.
Morgan Griffith, Principal Engineer, Exponent, Menlo Park, CA, USA.
Brian McDonald, Corporate Vice President and Principal Engineer, Exponent, Menlo Park, CA, USA.

INTRODUCTION

Wildfires in California result in millions of acres burned per year, causing property destruction and, in extreme cases, fatalities [1]. Some of these fires have been attributed to equipment failures of electrical transmission and distribution infrastructure [2,3]. This paper describes an electrical infrastructure monitoring framework to mitigate wildfire risk. A case study is presented that illustrates the impact that the hazard modeling approach can have on the framework output. The goal of the framework is to incorporate first-principles modeling, historical performance data, inspection data, and other information about assets of an electrical infrastructure system to direct inspection and maintenance efforts in order to prevent component failures that could result in wildfire ignition.

OVERVIEW OF FRAMEWORK METHODOLOGY

First, a database of assets (i.e., structures and their supported conductors and equipment) is created. This database includes information about component type, age, material, and environmental conditions. With this information, the structural capacity of each asset can be estimated and projected forward in time to track expected performance against various hazards as the asset ages and deteriorates. In this paper, wind hazards are considered, but the methodology has also been adapted to earthquakes and other hazards. Based on historical wind records, the annualized probability of failure for each asset is estimated. With this model, both current and future annualized probabilities of failure can be estimated to characterize long-term asset health and coordinate future interventions.

CAPACITY CALCULATION

For wind hazards, the capacity of each asset is modeled as a fragility function, which estimates the asset's conditional probability of failure as a function of windspeed (Figure 1). Each fragility function is parametrized as a lognormal cumulative distribution function (CDF) with a median, the windspeed at which half of all assets would fail, and a dispersion parameter, β. Fragility functions are developed based on target reliabilities from standards for reliability-based design of transmission structures [4, 5]. Median strengths are determined by assuming that all components are designed to the minimum design wind loads for transmission structures given by California Public Utilities Commission General Order 95 (GO 95) [6]. To account for the condition of the asset in the field, these base fragility curve parameters are modified based on a structure's age, first-principles degradation models, observations of field condition, and historical power outage records.

As an asset ages, uncertainty in the asset's ability to resist load increases, modeled as an increase in the dispersion parameter. For each asset type, a design life is assumed, beyond which the asset should be evaluated, repaired, or replaced. At the design life, a dispersion is selected that produces a conditional probability of failure at the design windspeed corresponding to a 1/3 reduction in asset strength. This 1/3 factor was se-

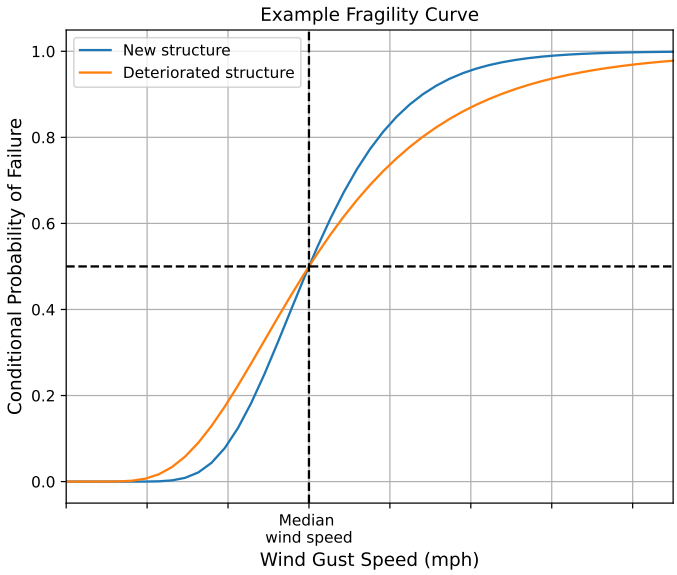

Figure 1. Example fragility function for new and deteriorated structures.

lected to reflect the GO 95 standard, which mandates intervention when the "at new" safety factor drops below 2/3. The dispersion, β, is assumed to follow a parabolic function between the starting dispersion, β_0, and the dispersion at the design life, β_R (Figure 2). However, these values do not account for additional deterioration due to environmental effects. First-principles degradation models, termed threat models, further modify the fragility curve for a given asset over time to account for reductions in strength and increasing uncertainty in performance. Examples of threat models that have been addressed include atmospheric and underground corrosion, fatigue, and wear. The threats are specific to each site; for example, the corrosion threat at a given site is based on available environmental records. Threats typically modify the design life, which in turn modifies the dispersion, affecting asset strength uncertainty.

Field inspection and historical performance data are also considered in the model. For example, standardized inspections of wood pole decay are mapped to incremental strength reductions, which modify the median strength. Historical performance records are incorporated through a Bayesian updating procedure. Prior distributions are assumed for the fragility median and dispersion. These distributions are updated considering historical power outages and maximum daily windspeeds. Note that with Bayesian updating, strength and uncertainty can either increase or decrease. The final fragility function for each asset accounts for age, threat models, inspection data, and Bayesian updating modifiers.

HAZARD MODELING

The wind hazard model is developed from historical windspeed records. Provided with records of maximum daily 3-second gust windspeed, an empirical CDF of maximum daily windspeed is developed (Figure 3). A Type I Extreme Value (Gumbel)

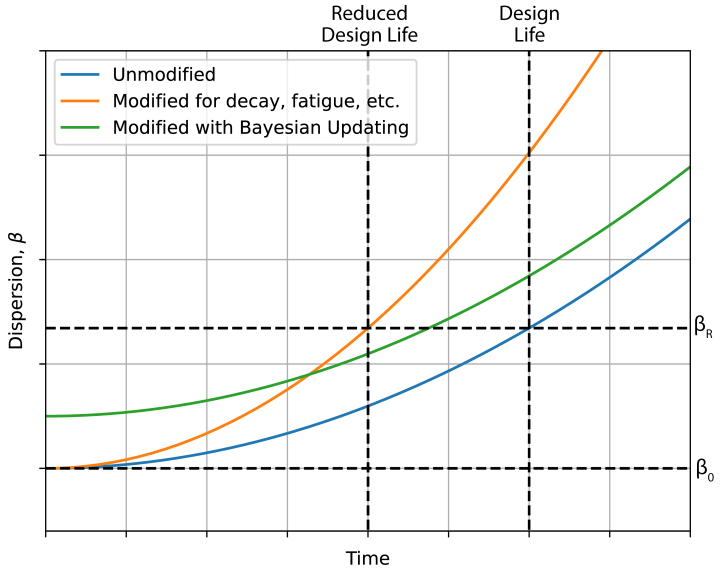

Figure 2. Fragility dispersion, β, as a function of time for different structures subject to different capacity modifications.

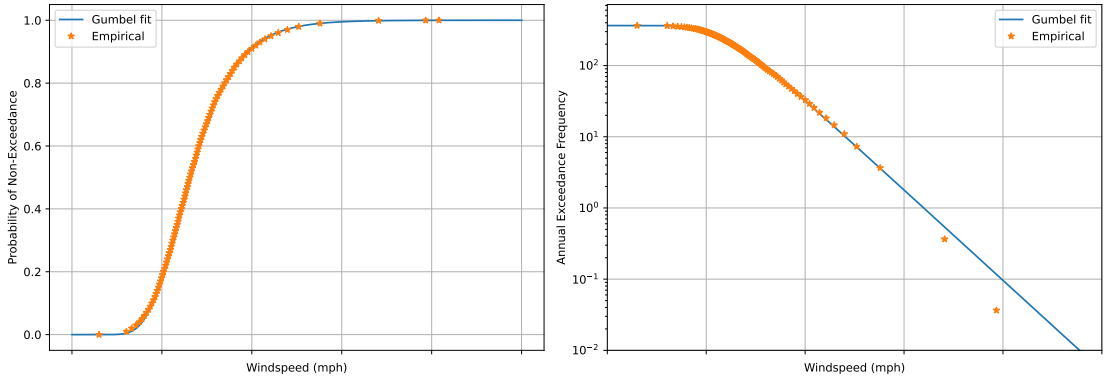

Figure 3. Example maximum daily windspeed CDF (left) and associated hazard curve (right).

distribution is fit to this empirical CDF. From the Gumbel CDF, annual exceedance frequencies are calculated to produce a hazard curve for annualized probability of failure calculations. Note that an empirical hazard curve could also be developed from the windspeed data directly. However, fitting an analytical hazard curve enables efficient characterization of wind hazards across many thousands of sites, and accounts for the possibility of higher windspeeds than those of the historical record.

ESTIMATING ANNUALIZED PROBABILITY OF FAILURE

Given an asset fragility function and hazard curve, the annual failure rate, λ, is calculated:

$$\lambda = \int_0^\infty p(f|im) \left| \frac{dh}{dim} \right| dim \tag{1}$$

where, im is the hazard, $p(f|im)$ is probability of failure conditioned on the intensity of the hazard (the fragility function), and $\left|\frac{dh}{dim}\right|$ is the absolute value of the derivative of the hazard curve. Assuming failures follow a Poisson process, the annualized probability of failure is given by:

$$P(f) = 1 - e^{-\lambda} \tag{2}$$

The annualized probability of failure is computed for each asset in the system. These probabilities are communicated to stakeholders to help direct maintenance and repair operations. The predictions can also further be refined as new inspection data becomes available or new components are installed. The results, however, are sensitive to modeling decisions and assumptions for each aspect of the model. The following section investigates how the resulting annualized probabilities of failure can be impacted by the choice of hazard curve modeling.

CASE STUDY: HAZARD CURVE MODELING IMPACTS ON ANNUALIZED PROBABILITY OF FAILURE

As described previously, the wind hazard at each site is described by a Gumbel distribution fit to historical maximum daily windspeed records. The Gumbel distribution provides a rational way to efficiently characterize wind hazard across many different sites; however, the quality of this fit can create bias in the predicted annualized probabilities of failure. Here, quality of fit is measured as the mean square error (MSE) between the empirical windspeed percentiles and the Gumbel distribution fit to the data. Three example windspeed CDFs are shown in Figure 4. At Site A, the Gumbel distribution underestimates the windspeed percentiles at higher windspeeds. Consequently, calculations with the Gumbel hazard curve will overestimate the annualized probability of failure. In contrast, at Site B, the Gumbel distribution overestimates the windspeed percentiles at high windspeeds. Consequently, this hazard curve will underestimate annualized probability of failure for that site, potentially obscuring high-risk assets in the system. At Site C, the MSE value is several orders of magnitude lower than that of either A or B, and the Gumbel distribution approximates the empirical windspeed percentiles very closely. This variability across sites can result in geographically biased estimates of annualized probabilities of failure.

To evaluate the impact of hazard curve fit, the equivalent annualized probability of failure metric is introduced. The purpose of this metric is to account for the variability in windspeed magnitude across different sites (i.e., the natural variability in site windiness). At each site, an empirical hazard curve is considered, based on historical windspeed data. An asset fragility function is found that yields an annualized probability of failure of 0.001 (chosen for convenience) when integrated with that site's empirical hazard curve. The equivalent annualized probability of failure at a site is obtained when integrating this fragility function with the Gumbel distribution for that site. Thus, the equivalent annualized probability of failure normalizes each site to a uniform annualized probability

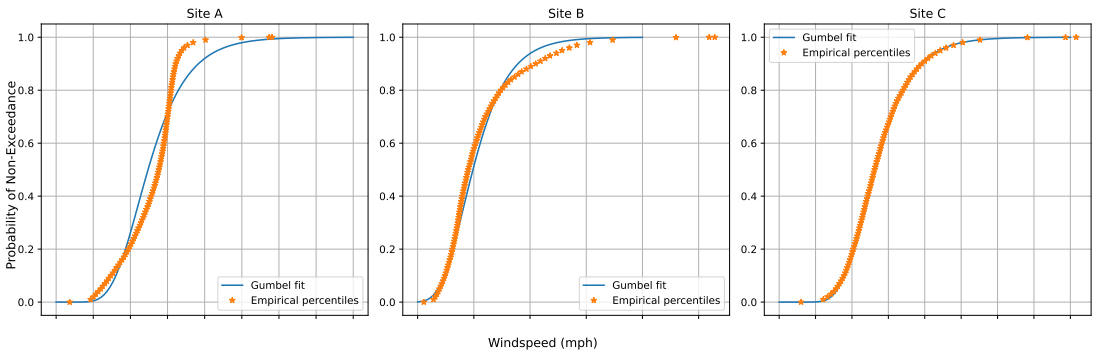

Figure 4. Empirical and Gumbel fit maximum daily windspeed CDFs for different sites.

of failure for the empirical wind hazard so that the impact of the hazard curve fit can be compared across different sites.

The equivalent annualized probability of failure is computed for each asset along an example transmission line. Mapping the distribution of both MSE and equivalent annualized probability of failure along the line reveals geographic bias solely due to hazard curve fit quality. The following section presents the mapped equivalent annualized probabilities of failure and discusses implications for the risk model.

RESULTS AND DISCUSSION

The MSE and the equivalent annualized probability of failure for each asset of the example transmission line are plotted geographically in Figure 5. Each asset on the map is represented with a single marker. The example transmission line trends approximately east-west. MSE values are low to moderate along most of the length, except at the east end, where MSE is highest. Ideally, each asset will have an equivalent annualized probability of failure slightly higher than 0.001. This result would indicate that the Gumbel distribution provides a good approximation of the empirical hazard curve, but also captures the additional risk due to the possibility of windspeeds greater than the highest measured historical windspeed. However, as Figure 5 shows, the equivalent annualized probability of failure ranges over several orders of magnitude, from a minimum of 3.1×10^{-5} to a maximum of 0.26 for the example line. These extreme values typically occur near transitions between types of topography, such as mountain passes. Note that the magnitude of equivalent annualized probability of failure does not necessarily correlate with the magnitude of MSE. In other words, some assets with high MSE still have equivalent annualized probability of failure close to 0.001, and vice versa. This is likely because annualized probability of failure is driven by values at the upper tail of the hazard curve, while MSE considers the full range of windspeeds.

The poor analytical hazard curve fit, and consequent high variability in the equivalent annualized probability of failure, may be a result of varying environment and geography. For example, previous research has documented that wind maxima driven by different phenomena will follow different distributions [7, 8]. One possibility is that in these topographically complex regions, windspeed maxima are driven by multiple weather phenomena, and therefore a single Gumbel distribution cannot adequately describe the

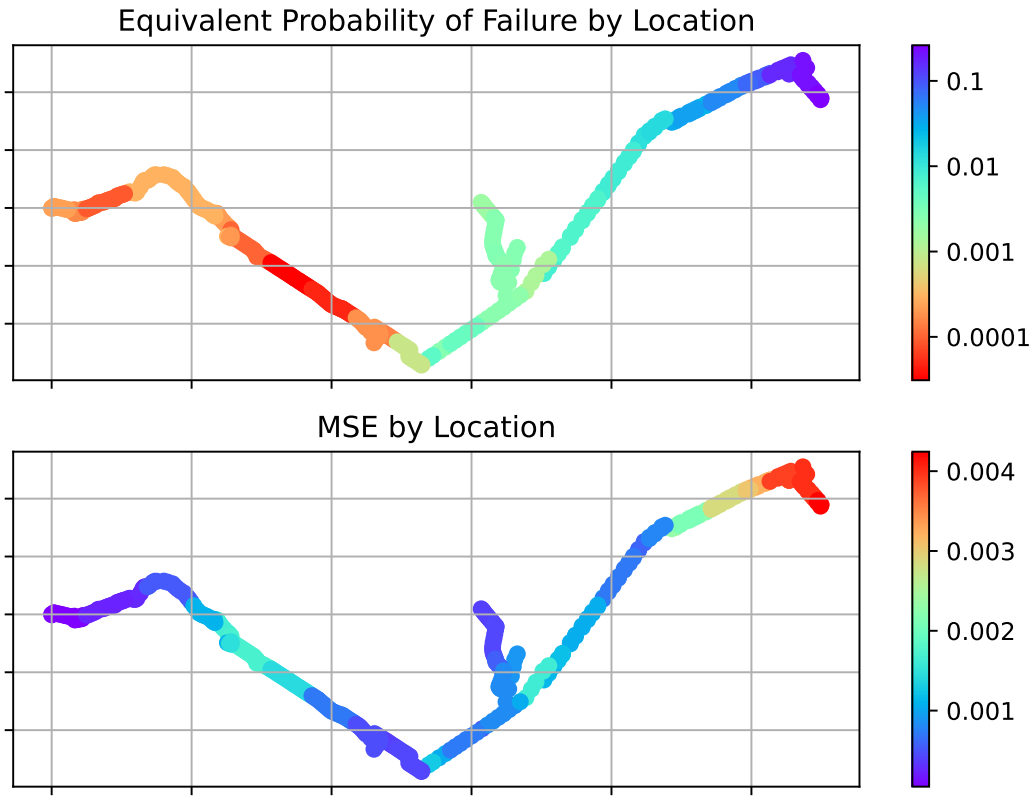

Figure 5. Equivalent probability of failure and MSE plotted along an example transmission line.

wind hazard. Regardless of the cause, the variability in equivalent annualized probability of failure presents challenges for the successful application of an electrical infrastructure management model.

This variability causes certain regions to have a bias towards lower or higher predicted annualized probabilities of asset failure. The model would seemingly predict better asset health in regions with a bias towards lower annualized probabilities of failure and worse asset health in regions with a bias towards higher annualized probabilities of failure. For example, assets in Figure 5 (top) with warmer colors could falsely appear to be in good condition, while assets with cooler colors could falsely appear to be in need of repair. If the model results are used to direct inspection and maintenance operations, this bias can direct resources towards assets in good condition and away from assets that require intervention.

CONCLUSIONS

This paper described a model developed to monitor large inventories of electrical infrastructure assets. Fragility functions were used to represent asset capacities; these functions were modified to account for age, environmental threats, historical performance, and inspection data. Wind hazard was represented by fitting a Gumbel distribu-

tion to an empirical CDF developed from site-specific historical wind data. The consequences of this approach were investigated, and in some cases it was found to produce geographic bias in the predicted annualized probabilities of asset failure. This bias could result in resources being redirected away from deficient assets in need of maintenance. Ongoing efforts will explore different ways of capturing this hazard, such as using the peaks-over-threshold method to fit a Generalized Pareto Distribution to the upper tail of the empirical wind data [9]. Such a method may produce more consistent annualized probabilities of failure across sites.

REFERENCES

1. CalFire. 2023. "Current Emergency Incidents," *https://www.fire.ca.gov/incidents/*.
2. Penn, I. 17 Oct 2017, "Power lines and electrical equipment are a leading cause of California wildfires," Los Angeles Times, available: https://www.latimes.com/business/la-fi-utility-wildfires-20171017-story.html, accessed: 11 May 2023.
3. Moon, S. 5 Jan 2022, "California's second-largest wildfire was sparked when power lines came in contact with a tree, Cal Fire says," CNN, available: https://www.cnn.com/2022/01/05/us/dixie-fire-power-lines-cause-pge/index.html, accessed: 11 May 2023.
4. Criswell, M. and M. Vanderbilt. 1987. "Reliability-Based Design of Transmission Line Structures: Final Report," *EPRI EL-4793*:1352–2.
5. Dagher, H. J. 2006. "Reliability-based design of utility pole structures," American Society of Civil Engineers Reston, VA.
6. California Public Utilities Commission. 2020. *General Order No. 95 Rules for Overhead Electric Line Construction*, State of California.
7. Gomes, L. and B. Vickery. 1978. "Extreme wind speeds in mixed wind climates," *Journal of Wind Engineering and Industrial Aerodynamics*, 2(4):331–344, ISSN 0167-6105, doi:https://doi.org/10.1016/0167-6105(78)90018-1.
8. Cook, N. J., R. I. Harris, and R. Whiting. 2003. "Extreme wind speeds in mixed climates revisited," *Journal of Wind Engineering and Industrial Aerodynamics*, 91(3):403–422.
9. Holmes, J. D. and S. Bekele. 2020. *Wind Loading of Structures*, CRC Press, 4 edn.